# A study on the influence of Ni-Ti M-Wire in the flexural fatigue life of endodontic rotary files by using Finite Element Analysis

Diogo Montalvão[a,*], Qiu Shengwen[a], Manuel Freitas[b]

[a] School of Engineering and Technology, University of Hertfordshire, College Lane Campus, Hatfield, Herts, AL10 9AB, UK.

[a] Instituto Superior Técnico, Technical University of Lisbon, Av. Rovisco Pais, 1, 1049-001 Lisboa, Portugal.

## Abstract

The aim of this paper is to analyze the cyclic performance of two different Ni-Ti endodontic rotary files made from different alloys under bending using Finite Element Analysis (FEA). When experimentation is not available, this is not a trivial task and most papers on the subject rely on static analysis only. Two Ni-Ti rotary instruments are selected, ProFile GT and a GT Series X (GTX). The latter file is made from M-Wire, which has been thermo-mechanically processed to have larger flexibility, according to its manufacturer. The mechanical response was studied by considering different scenarios in the FEA package, in which the material properties were introduced according to existing literature. The method and results are presented and discussed so that this paper can be used as a guideline for future works. Although not fully reflective of the instrument's behavior in a dynamic rotation intra-canal system, the models used constitute a good approximation when a comparison between two instruments is at stake. It is shown that the GTX file has a lower risk of fatigue fracture during

* Corresponding author: Tel.: +44 (0) 1707 285 387.
e-mail address: d.montalvao@herts.ac.uk.

its clinical use when compared to the GT file, especially when the root canal makes the file deform into an extreme geometry. However, if the root canal does not make the file deform more than a certain amount, the GT file is equally good from the point of view of mechanical endurance.

**Key Words**

Ni-Ti Rotary file; Endodontic instrument; Cyclic Loading; Fatigue; M-Wire.

## 1. Introduction

Endodontic rotary instruments are used to remove the inflamed or necrotic pulp tissue from the root canal in the conventional endodontic treatment. However, the morphology of the root canal system and the curvature of the roots vary, and these factors provide great challenges for dentists [1]. Nickel-titanium (Ni-Ti) alloys have been used in endodontic rotary instruments for the past 30 years, gradually replacing stainless steel files due to superior performance in the root canal treatment [2]. Compared with the stainless steel rotary instrument, Ni-Ti files have superior flexibility properties due to the Ni-Ti unique property of super elasticity. Ni-Ti rotary instruments can follow curved root canals more easily than stainless steel instruments [3]. Also, Ni-Ti files are more effective in the removal of the inflamed pulp tissue and protection of the tooth structure, as flexibility preserves dental structure, limits apical transport, reduces the risk of iatrogenic mistakes and, ultimately, allows for irrigants to flow deeper in canals towards the apical constriction [2,4]. Moreover, some studies show that Ni-Ti alloys have superior ductility, fatigue resistance, recoverable strain, biocompatibility and corrosion resistance properties than their stainless steel counterparts [5].

Ni-Ti alloy is often referred as a Shape Memory Alloy (SMA). SMAs have the ability to recover shape when temperature increases [6]. In this process, there is a crystallographic phase

transformation from martensite to austenite. In addition, under specific conditions, mechanical energy can be absorbed and dissipated by undergoing a reversible hysteretic loop when applying cyclic loads. The SMAs have two basic properties: shape memory effect and pseudo elasticity.

However, fracture of instruments used in rotary motion has been reported. Generally, it occurs in two different ways: fracture caused by torsion and by flexural fatigue [7]. Torsional facture occurs when the instrument is locked in the root canal while the shank continues spinning. When the applied torque exceeds the elastic limit of the metal, fracture is inevitable [8]. Some motors already bring safety mechanisms that will prevent fracture by torsion, with automatic stop-reverse functions in the case of twist lock.

Fracture caused through flexure occurs due to metal fatigue [9]. The rotary file spins inside the root canal, generating variable traction/compression loads that shift with rotation at each location. In other words, at a given moment, parts of the instrument shaft are subjected to traction loads, whereas other parts are subjected to compressive loads. The oscillation between traction and compression loads leads to cyclic fatigue of the instrument over time and is acknowledged as an important factor in instrument fracture [10].

Stainless steel instrument often present visible signals of degradation before fracture (mostly by plastic deformation), but fracture of the Ni-Ti files is difficult to be noticed due to its super-elasticity. Hence, Ni-Ti files present a higher risk of fracture inside the root canal during clinical use than stainless steel instruments.

Recent developments have improved the properties of rotary instrument files by using new alloys with special thermal treatments and manufacturing processes [11]. For example, the GT Series X (GTX) from Dentsply Tulsa Dental Specialties are manufactured using a heat-treated Ni-Ti wire called M-Wire [12]. Reported results suggest that GTX instruments are more resistant to flexural fatigue than similar GT instruments made with conventional Ni-Ti alloys

[13,15]. However, due to the files' small size (less than 1mm in diameter), it is very hard to measure with accuracy important mechanical properties that will contribute to fracture by fatigue, for instance the stress at a given location. First, it is very hard to find strain sensing technology in the market (if any). Secondly, when subjected to stress under bending, the file's crystallography is very heterogeneous along each section and the material is no longer isotropic or with linear behavior [16].

Computational methods, as Finite Element Analysis (FEA), can be used to describe the mechanical behavior of these instruments (e.g. the stress distribution) and predict the most likely to be location for crack growth. This is very difficult to assess through laboratorial or in vivo tests [17].

There are several FEA studies in which files are compared, for example [14, 15, 18-21]. However, most of these consider static loads only. In such cases, the multi-linear kinematic hardening plastic material model are usually considered in the software to approximate the stress-strain relationship of the Ni-Ti alloy. However, this material model does not allow to include hysteresis, which is quite significant for SMAs.

The purpose of this study is to evaluate how different Ni-Ti alloys - conventional and M-Wire - determine the cyclic performance of endodontic rotary files. Two types of endodontic rotary instruments with different NI-Ti alloys are selected: ProFile GT 20/0.06 (GT) and GT series X 20/0.06 (GTX). To obtain a comprehensive comparison of their mechanical performance, both elastic responses and plasticity effects are evaluated. The deformation and stress distributions are determined in a series of FEA simulations, including static bending and cycling loading. For a matter of comparability with other studies, the same load and boundary conditions than those used in other works were selected [19-21]. Validation was done with experimental tests in which the files were clamped and subjected to pure bending.

## 2. Materials and methods

*2.1. Specimens*

Two commercially available Ni-Ti rotary instruments with different cross-section geometries and materials are selected for this study: ProFile GT 20/.06 (GT) and GT series X 20/.06 (GTX). In this chapter, the geometrical models of both instruments, mesh method, mechanical properties, and computational setup are discussed.

*2.2. Geometrical Models*

A Mitutoyo PJ-A300 with QM Data 200 profile projector and a Leica Zoom 2000 microscope were used to assist in the geometric characterization of both the GT and GTX files. The objective is that the CAD geometrical models resemble the real files as much as possible, including variable radial land widths along the instruments' active parts.

Usually, the file can be divided into three main parts: handle, shaft and blade. The total length of both files compared in this study is 17 mm with a 14.3 mm long working part. In addition, both instruments have a 1 mm diameter at the transition section between the shaft and blade and approximately 6% taper. However, there are some differences between the GT and GTX files, which are shown in the figure 1. Compared with the GT file, the GTX has fewer spirals because of its larger pitch length. Besides, the pitch length of both the GT and GTX files are variable. The CAD models were created in CATIA V5. The proposed models, shown in figure 1, accurately reproduce the actual dimensions of the working part of the instruments, which can be seen from the superposition of the models' edges over the photos, including different triple u-shaped cross-sections and variable land widths.

Comparing with previous reports, more details are considered in these models. For the GT system, the variations in pitch length are 4 mm, 3.5mm, 2.5mm and 2mm, arranged in an arithmetic sequence. For the GTX system, the variation on the pitch length of each helix is 6.4

mm, 5.4 mm and 3.4 mm. In addition, the smooth transition between different sections of the file are also considered to improve the accuracy of the models. In addition, although the GT and GTX instruments have similar cross-sections, there are some differences as shown in figure 1 (the angles of adjacent cutting edges of the GT instrument, 16.5°, are larger than the 12° in the GTX instrument).

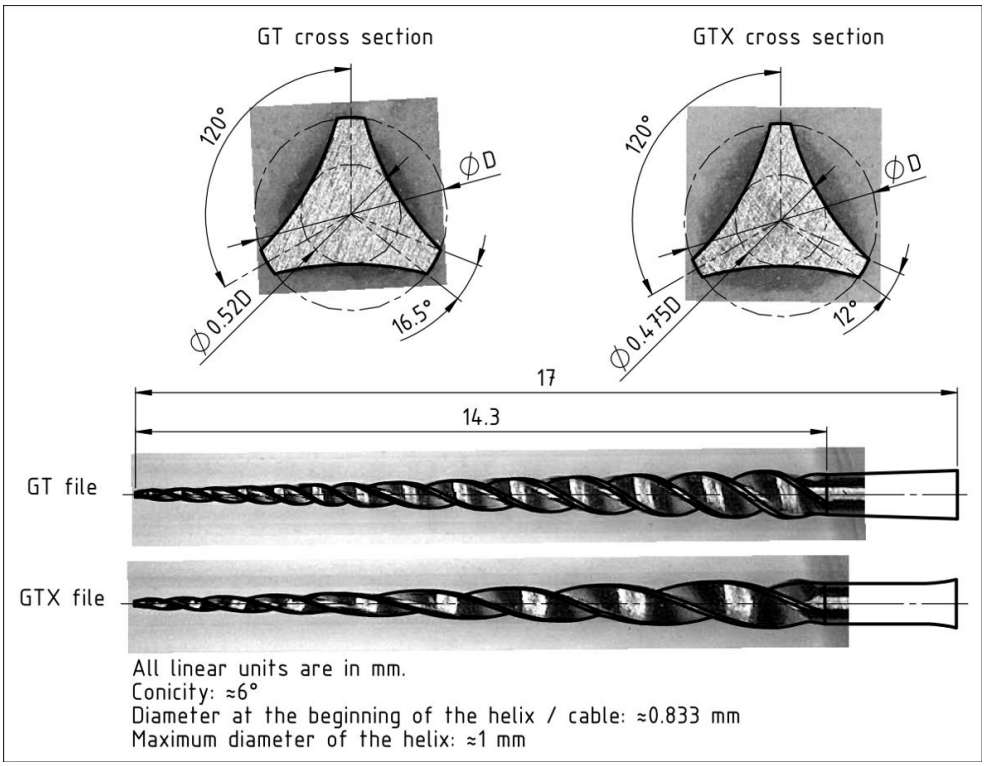


**Figure 1.** Cross-sectional and longitudinal geometries of the GT and GTX file instruments used in this study, where *D* stands for the local diameter.

*2.3. Mesh*

The 3D geometrical models were meshed using Solid 186 in ANSYS. Solid 186 is a higher order 3-D 10 node tetrahedral structural solid element which has quadratic displacement behavior and is well suited to model irregular meshes. This element also supports hyper-elasticity, large deflection and large strain capabilities, which are very important properties for SMAs.

In this study, a refined mesh was used in order to improve the accuracy of the results. The final FE models of the GT and GTX instruments consist of 2744 elements with 5665 nodes and 3199 elements with 6517 nodes respectively.

*2.4. Material Models*

The multi-kinematic hardening plastic material model has been used by other authors before [14, 19] to approximate the stress-strain relationship of the Ni-Ti alloy when modeling Ni-Ti rotary files. The multi-kinematic hardening plastic material model can include the super-elasticity behavior of the Ni-Ti alloy from stress-strain data. However, it is not suitable to describe the hysteresis loop observed during unloading, which is very important in SMAs. Hence, differently from the aforementioned papers, the properties of the Ni-Ti alloy will be modeled using the SMA option in ANSYS. The SMA option is described by six constants that define the characteristic of the stress-strain curve in loading and unloading for the uniaxial stress-state. This model is more suitable to analyze cyclic loading than the multi-kinematic hardening plastic material model because it includes hysteresis, although the material's behavior characterisation is slightly coarser.

When under uniaxial cyclic loading, SMAs behavior can be divided into two phases in a stress *vs* strain plot: the forward phase and the reverse phase. The forward phase, indicating the stress-strain relationship of the Ni-Ti alloy during loading, may be subdivided into three parts. The first part is linear, in which the Ni-Ti alloy presents a more stable crystalline phase, of the austenitic type. The second part of the plot is also linear but with a much smaller slope than the first part, during which the material is in transition from the austenitic to the martensitic phase. This transition phase is often referred in the literature as phase-R [22, 23], in which for a very small change in load a large strain is produced. This characteristic of the material is what is generally identified as pseudo-elasticity and is seen in a stress *vs* strain chart as a plateau.

The third part, also linear and again steeper, is characterized by a martensitic crystallographic phase. On the reverse phase, the transformation between martensitic phase and austenitic phase starts and finishes when the load is removed. Just like the forward phase, the reverse phase can also be divided into three parts. However, the stress plateau is now at a much lower stress level than during loading. This is because the SMA present a very large hysteresis loop.

Regarding the instruments being studied in this work, the major differentiating factor between the GT and GTX files, in terms of Mechanical performance, is not expected to be the geometry alone, but the use of different alloys. As discussed in the introduction section, the GTX is produced using a heat-treated Ni-Ti wire called M-Wire. This M-Wire, which is also used in other endodontic files, is suggested to have greater resistance to fatigue than the conventional instrument (e.g. GT file) [24].

In this work, the material properties are modeled from the stress-strain relationships found in the literature [25]. First of all, it is assumed that each one of the three parts in the stress-strain plots (Austenitic, Phase-R and Martensitic) in [25] can be reasonably well approximated by linear relationships. Having this into consideration, the slope of the M-Wire alloy is smaller than that of the conventional Ni-Ti alloy during the elastic austenitic phase (approximately 23.5 GPa against 34.3 GPa). It also begins the transformation phase (the pseudo-elastic plateau) at a lower stress when compared to convetional Ni-Ti alloy (around 448.2 MPa against 482.6 MPa). Finally, the M-Wire alloy has smaller stress at the end of the transformation phase (551.6 MPa against 620.5 MPa). On the other hand, the limit transformation strain for the M-Wire Ni-Ti alloy seems to be shorter than that of the conventional Ni-Ti alloy from the plots in [25] (6.8% against 4.5%). These values of characteristics parameters are imported into the SMAs model in ANSYS (table **1**).

**Table 1.** SMA constants according to the material properties from [25].

| Constant | Symbol | Unit | Value | |
|---|---|---|---|---|
| | | | GT | GTX |
| Starting stress value for the forward phase transformation | $S_s^{AS}$ | MPa | 482.6 | 448.2 |
| Final stress value for the forward phase transformation | $S_f^{AS}$ | MPa | 620.5 | 551.6 |
| Starting stress value for the reverse phase transformation | $S_s^{SA}$ | MPa | 379.2 | 344.7 |
| Final stress value for the reverse phase transformation | $S_f^{SA}$ | MPa | 103.4 | 137.9 |
| Maximum residual strain | $e_L$ | % | 6.8 | 4.5 |

The strain-life parameters for the fatigue analysis were introduced in ANSYS based on [26,27]. As far as the authors are concerned, this data has never been determined for the specific instruments under study in this work, so the same parameters were considered when modeling both files. These parameters are shown in table 2. Finally, Poisson and density were defined as 0.33 and 1500kgm$^3$ respectively [28].

**Table 2.** Representative parameters for the fatigue behavior of Ni-Ti alloys [26,27] – Stain-life model.

| Constant | Unit | Value |
|---|---|---|
| Strength coefficient | MPa | 705 |
| Strength exponent | | -0.06 |
| Ductility coefficient | | 0.68 |
| Ductility exponent | | 0.6 |
| Cyclic strength coefficient | MPa | 733 |
| Cyclic strain hardening exponent | | 0.1 |

*2.4. Loads and Boundary Conditions*

In this study, the file is treated as a cantilever beam with a force applied at its tip. The mechanical behavior of both the different files is determined by using ANSYS software. Two simulations were carried out:

1. Simulation 1: Deflection of the instrument tip is measured and the Von Mises stress distribution is assessed after applying a 1 N static load at the tip when its shaft is clamped (figure 2).
2. Simulation 2: Evaluation of fatigue life assessment in bending cyclic loading under a 1 N rotating load.

Real instruments are inserted into the root canal while rotating, which involves cyclic bending. This process is complex to model in an FEA package. Hence, a simplification process, which is based on the quasi-static simulation (simulation 1), is followed: the 1 N load is a rotating force that is applied at the tip of the instrument from different directions in the *yz* plane. The first 10 steps correspond to the iNi-Tial bending (as in simulation 1). Then, each rotational cycle is completed after 40 sub-steps. At each ten steps the load is applied at a perpendicular direction to the direction ten steps earlier. This process is then repeated at each 40 steps. The plot of the load *vs* timestep for one complete rotational cycle is shown in figure 4, in which it can be seen that during the first 10 steps the load is applied linearly at one direction only (*y*), whereas during the next 40 rotational steps the load is applied as a sinusoidal at two orthogonal directions simultaneoulsy (*y* and *z*). During the rotational application of the load, its amplitude is fixed at 1 N.

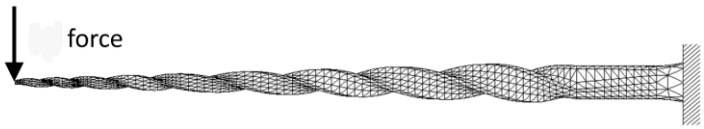


**Figure 3.** Example of the boundary conditions applied at the GTX file.

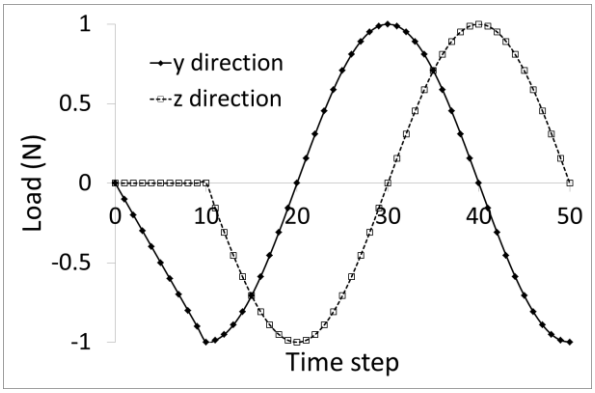


**Figure 4.** Load time steps to simulate the bending of the file inside the root canal after one rotation cycle.

*2.5. Experimental Validation of the Numerical Results*

For the experimental validation of the numerical results, tests have been conducted in a similar way to simulation 1 described in the previous section. Files were subjected to an increasing force at the tip, up to 1 N, while the shaft was clamped to an aluminum fixture. A force *vs* displacement plot was traced during both the loading and unloading cycles and the maximum loads and displacements were recorded. Three GT and three GTX files were selected, and tests were conducted three times per file. Force and deflection were measured using a Sauter test rig, composed by an FN-10 digital force gauge (10N range with a 0.005 N resolution) and a TVL manual test stand equipped with a displacement gauge with 0.01 mm resolution. A triangular probe was used to apply the load at the tip.

Endodontic file instruments are designed to be used at body temperature, which is 37° C approximately [29]. Endodontic files were heat up to body temperature with a a Bosch hot air

gun D-70745, since room temperature was at ~20° C at the time the experiment was run. A Fluke thermography camera Ti25 was used to continuously monitor and map the temperature of the file during the experiments. However, because the Ni-Ti rotary endodontic files are very small (with a diameter smaller than 1 mm), the camera's resolution is not enough to capture the file's actual temperature. Thus, the temperature of the probe was used as control temperature. The hot air gun temperature was adjusted in order to keep the probe's temperature stable and homogeneously distributed at approximately 37 °C, as can be observed in the thermography sample image presented in figure 5.

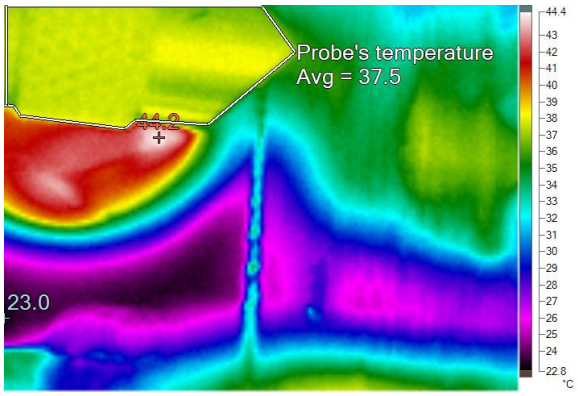


**Figure 5.** Thermography image of the GT file taken with the Fluke camera.

## 3. Results

*3.1. Simulation 1 – Static Bending and Experimental Validation*

In simulation 1, a 1 N force is gradually applied at the tip of the file and then it is gradually released, while its shaft is clamped. Figure 6 shows the Von Mises stress distribution along the file for each instrument. The maximum Von Mises stress values obtained for the GT (left) and GTX files (right) were 555 MPa and 488 MPa, respectively, which are in agreement with the values obtained in a previous simulation using a different material model [14]. On the other

hand, it can be found that tip deflection in the GTX instrument is larger than that of the GT instrument under the same load (7.89 mm against 6.89 mm).

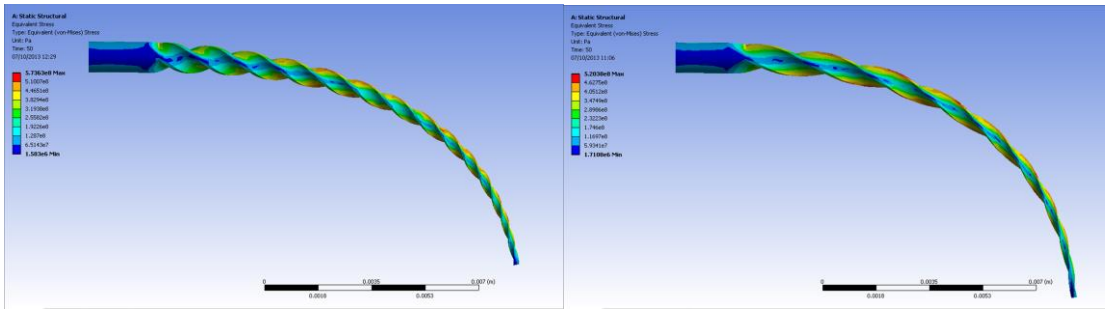

**Figure 6.** Bending deflection and Von Mises stress distribution of the GT (left) and GTX (right) files under a 1 N force applied at the tip.

Although similar, the GT and GTX files present some geometrical differences, besides the material. In order to assess how the M-Wire actually conditions the GTX behavior, a simulation was run where the GTX was modeled with the same material properties as the GT file (table 1). In this simulation, a maximum Von Mises stress of 529 MPa and a deflection of 6.99 mm were obtained. Both these values are closer to the ones obtained for the GT file, especially the deflection. This supports the suggestion that the GTX is more flexible than the GT mainly due to the differences in the material properties, rather than in the geometry itself.

Validation of the Finite Element Models (FEMs) was done by means of an experiment in which the file was treated as a cantilever beam (same as described in section 2.5). Plots of the force *vs* displacement results obtained with the FEM and experimental tests at two different temperatures (room and body temperature) are shown in figure 7. A summary of the results is shown in table 2.

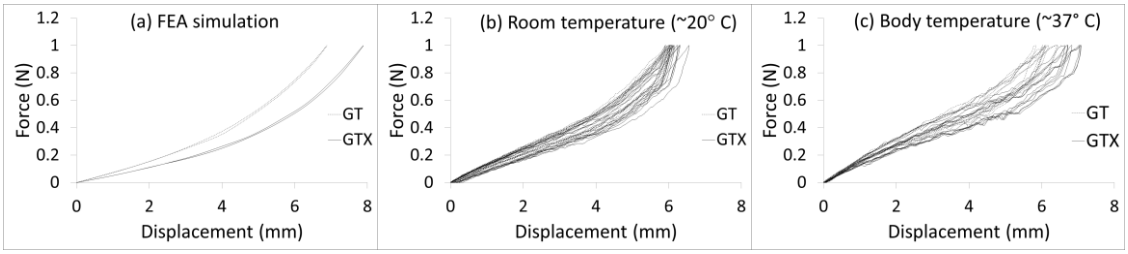


**Figure 7.** Bending force *vs* deflection (measured at the tip) for both files GT and GTX: (a) FEM simulation results; (b) experimental results at room temperature (20 °C); (c) experimental results at body temperature (37 °C).

**Table 2.** Maximum deflection at the tip obtained in the FEM simulation and experimental tests for both the GT and GTX files.

| File | FEA | Room temperature (20 °C) | | | Body temperature (37 °C) | | |
|---|---|---|---|---|---|---|---|
| | Deflection | Average Deflection | Standard Deviation | Error | Average Deflection | Standard Deviation | Error |
| GT | 6.89 mm | 6.01 mm | 0.071 mm | 12.8% | 6.15 mm | 0.199 mm | 10.7% |
| GTX | 7.89 mm | 6.23 mm | 0.160 mm | 21.0% | 6.87 mm | 0.190 mm | 12.9% |
| Δ | +12.7% | +3.5% | | | +10.5% | | |

In general, it can be observed that the GT instrument has a larger stiffness than the GTX instrument, as it presents a smaller deflection under the same load. Moreover, the stiffness curves of both instruments are non-linear, as expected, due to the materials' non-linear properties. Hysteresis is observed as well, due to the differences in the Ni-Ti material behavior during loading and unloading, although this is not as visible in the FEM results. This is explained below.

The GTX file showed to be more flexible than the GT in any scenario: simulated, room temperature and body temperature. However, at room temperature the difference is not as

large (3.5%) as at body temperature (10.5%). This is because of the optimal working temperature of the files.

The simulation produced considerably larger displacement values than the experimental tests, with differences up to 21%. For example, comparing the FEM results with those obtained experimentally at body temperature, the GTX file deflection at the tip is 12.9% smaller. At first, reasons for these discrepancies could be related to the simplified material models used in the FEM. However, there are some experimental issues that, if taken into consideration, may explain why such large differences have been found:

- Body temperature was achieved using a hot air gun and heat was introduced through convection. This process is unstable and it does not guarantee a constant temperature profile across the file's cross section. This is supported from the comparison between graphs (b) and (c) in figure 6, in which plots at (b) are smoother and "steadier" than at (c). Furthermore, the standard deviation is larger for the results obtained at 37 °C.
- Large deformations are occurring. As a consequence, the file tip's displacement has the shape of an arc (it cannot be approximated by a vertical straight line, as it would be assumed for small deformations). Figure 8 shows the file and probe immediately before the test and during application of the force. It can be seen that the force application point is either distributed or shifted towards the direction of the clamp (to the left). Thus, for a load of 1 N and with the testing equipment available, it is understandable that the measured deformation is smaller than it would be in case the force could be kept applied at the tip at all times.

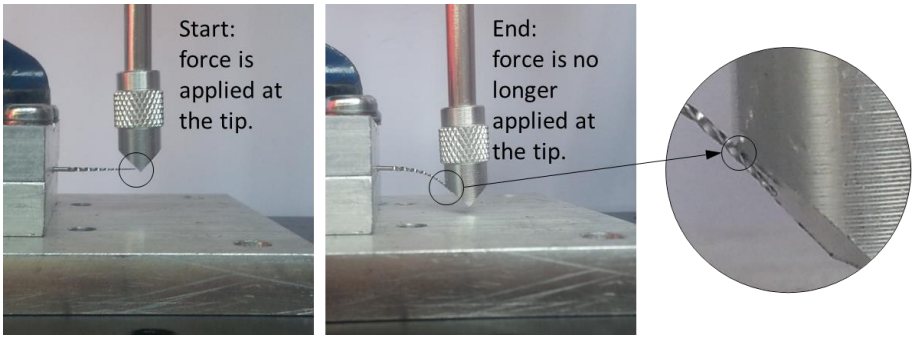


**Figure 8.** Change on the force application point during the experimental bending process.

- The large hysteresis observed in graphs (b) and (c) in figure 6 is accentuated because of the friction generated between the probe and the file. When the probe moves down (load cycle), a friction force is generated between the file and the inclined surface of the probe. This friction force will have opposing direction to the movement of the probe, thus increasing slightly the reading from the load cell. When the probe starts moving up (unload cycle), the friction force changes direction, thus decreasing slightly the reading from the load cell in comparison to the force being exerted at the file. This also helps explaining that the deflection of the file is smaller for a 1 N force than the one obtained in the FEM, since part of this force is being used to overcome friction.

In conclusion, even if the experimental results on table 2 are somewhat below the results obtained in the the FEA simulation, the understanding of the experimental limitations and the consistency of the order of greatness between numerical and experimental values show that these FEMs are fair approximations to the real files.

*3.2. Simulation 2 – Cyclic Bending*

Although the Ni-Ti alloys instruments allow relatively large bending deflection due to their super-elastic properties, repeated loading (cyclic loading) can lead to fatigue crack iNi-Tiation before reaching the yield stress. Hence, fatigue is a main failure mechanism for Ni-Ti alloy instruments, especially when used in highly curved canals.

It should be noticed that the Von Mises criteria is a formula that combines the 3 principal stresses into an equivalent stress. Hence, it does not differentiate between compressive and tensile stress. According to the results shown in section 3.1, it is already expected that the GT instrument may indicate a higher risk of fracture (i.e., earlier fracture) because of its larger stress amplitude when compared to the GTX.

The bending fatigue life of both the GT and GTX instruments has been determined considering the strain-life parameters from [26,27]. Infinite fatigue life was defined at $10^7$ cycles or above. Expressing the fatigue life in terms of the number of cycles may be meaningless for a dental practitioner. Thus, the results shown in figure 8 are expressed in minutes and assume that the Endodontic motor is rotating at 300 rpm, a speed that can be found in some motors available in the market. In this case, the infinite life is above 33 thousand minutes (or 550 hours) approximately.

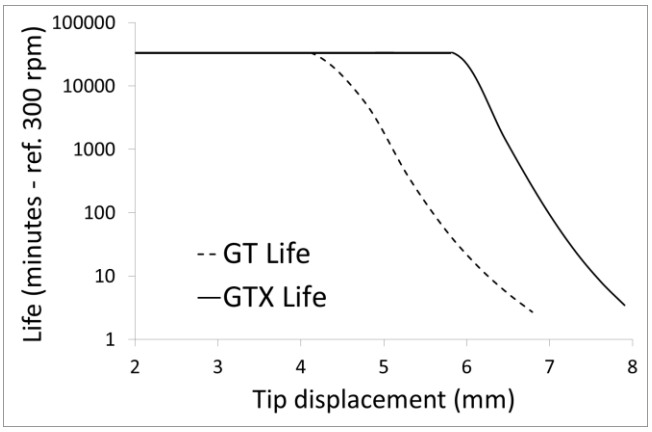


**Figure 9.** Bending fatigue life of both files GT and GTX expressed in terms of number of minutes *per* tip displacement in mm, for a motor running at a reference speed of 300 rpm.

According to these results, for displacements under 4mm both files will endure over 33 thousand minutes. Actually, the GTX is still capable of enduring infinite life up to 6mm tip deflection, approximately. However, displacements of 6~8mm at the tip of the file are quite large already, producing stresses that are not far away from Yield.

It must be highlighted that these results are numerical only. As such, a conservative approach is recommended when interpreting the data. First of all, the strain-life parameters that were used in the models are based on existing data from similar alloys that may not be exactly the same for the materials being tested in this study. Secondly, there are other variables that are not being taken into account in our models and that may be relevant during the clinical use of the files, for instance, friction, eventual gradients of temperature, complex root canal shapes, etc. Hence, the major conclusion is that the GT file made from "conventional" Ni-Ti seem adequate enough to treat root canals without the risk of premature fracture when the file is deformed under 6 mm at its tip in bending (according to these results, 6 mm allow up to 30 minutes of continuous use at 300 r.p.m. for the GT). For larger deformations and more winding canals, the GTX, made from M-Wire, is recommended. Also, if there is the possibility to sterilize the file in an autoclave and use it in the treatment of another patient, the GTX should be preferred to the GT file, at least from the point of view of prevention to fracture risk.

## 4. Conclusions

This study investigates how two different files can condition the risk of fracture of an endodontic file under cyclic loading, when inside the root canal during clinical use. This is assessed by means of FEA and considering that the deformation of the file inside the root canal can be approximated by a cantilevered beam subjected to a concentrated load at the tip. The Von Mises stress and deflection at the tip are evaluated. Furthermore, numerical results are validated with experimental results at simulated body temperature conditions (37 °C).

The main differences between the two investigated instruments are: material ("conventional" *vs* M-Wire Ni-Ti alloy), pitch length and cross-section. Generally speaking, it can be said that the GTX file is more flexible than the GT file under the same load conditions. Moreover, the maximum stresses observed on the GTX file are lower than on its counterpart GT file for the same load conditions. The cyclic bending simulations showed that the GT file has a higher risk of premature fracture than the GTX file, under the same load and boundary conditions. However, this does not mean that the GT file is not suitable for most endodontic treatments. This means that the GTX, for the same root canal configuration, will be able to endure more cycles than the GT instrument, especially when the file is subjected to significant deformation (>6 mm displacement at the tip when under bending). However, for root canals that are not very winding, both instruments are expected to be able to carry out the root canal treatment without significant risk of fracture, as long as the files are used in one dental treatment only.

**Acknowledgements**

The authors gratefully acknowledge financial support from FCT - *Fundação para Ciência e Tecnologia* - through the project PTDC/EME-PME/122795/2010.

## References


[1] Cohen S, Burns RC. Pathways of the Pulp. Elsevier Health Sciences, 8th Ed., 2001.

[2] Kell T, Azarpazhooh A, Peters OA, El-Mowafy O, Tompson B, Basrani B. Torsional profiles of new and used 20/.06 GT series X and GT rotary endodontic instruments. J Endod, 2009; 35:1278-1281.

[3] Walia H, Brantley WA. An initial investigation of the bending and torsional properties of Nitinol root canal files. J Endod, 1988; 14:346-351.

[4] Schäfer E, Oitzinger M. Cutting efficiency of five different types of rotary nickel titanium instruments. J Endod, 2008; 32:61-65.

[5] Pettiette MT, Delano EO, Trope M. Evaluation of success rate of endodontic treatment performed by students with stainless-steel K–files and nickel–titanium hand files. J Endod, 2001; 27:124-127.

[6] Kumar PK, Lagoudas DC. Introduction to Shape Memory Alloys. Springer Science+Business Media, LLC 2008.

[7] Grande NM, Plotino G, Pecci R, Bedini R, Malagnino VA. Cyclic fatigue resistance and three-dimensional analysis of instruments from two nickel-titanium rotary system. Int Endod J 2006; 39:755-763.

[8] Parashos P, Gordon I, Messer HH. Factors influencing defects of rotary nickel titanium endodontic instrument after clinical use. J Endod 2004; 30:722-725.

[9] Peter OA. Current challenges and concepts in the preparation of root canal system: a review. J Endod 2004; 30:559-565.

[10] Plotino G, Grand NM, Cordaro M, Testarelli L. Influence of the shape of artificial canals on the fatigue resistance of Ni-Ti rotary instruments. J Endod 2010; 43:69-75.

[11] Gambarini G, Gerosa R, Luca M, Garala M, Testarelli L. Mechanical properties of a new and improved nickel-titanium alloy for endodontic use: an evaluation of file flexibility. Oral Surg Oral Med Oral Pathol Oral Radiol Endod, 2008; 105:798-800.

[12] Alapati SB, Brantley WA, Iijima M, Clark WAT, Phil D, Kovarik L, Buie C, Liu J, Johnson WB. Characterization of a new nickel-titanium wire for rotary endodontic instruments. J Endod, 2009; 35:1589-1593.

[13] Johnson E, Lloyd A, Kuttler S, Namerow K. Comparisson between a novel nickel-titanium alloy and 508 Ni-Tinol on the cyclic fatigue life of ProFile 25/.04 rotary instrument. J Endod 2008; 34:1003-1005.

[14] Montalvão D, Alçada F. Numeric Comparison of the Static Mechanical Behavior between ProFile GT and ProFile GT Series X Rotary Nickel-Titanium Files. J Endod 2011; 37:1158-1161.

[15] Montalvão D, Alçada F, Fernandes FMB, Correia SV. Structural characterisation and mechanical FE analysis of conventional and M-Wire Ni-Ti alloys used in endodontic rotary instruments. Sci World J 2013; *In Press*.

[16] Chang YZ, Liu MC, Pai CA, Lin CL, Yen KI. Application of non-destructive impedance-based monitoring technique for cyclic fatigue evaluation of endodontic nickel–titanium rotary instruments. Med Eng Phys 2011; 33:604-609.

[17] Necchi S, Taschieri S, Petrini L, Migliavacca F. Mechanical behaviour of nickel-titanium rotary endodontic instruments in simulated clinical conditions: a computational study. Int Endod J 2008; 41:939-949.

[18] Berutti E, Chiandussi G, Gavilio I, Ibba A. Comparative analysis of torsional and bending stresses in two mathematical models of nickel-titanium rotary instrument: ProTaper versus ProFile. J Endond 2003; 29:15-19.

[19] Xu X, Eng M, Zheng Y, Eng D. Comparative study of torsional and bending properties for six models of nickel-titanium root canal instruments with different cross-sections. J Endod, 2006; 32:372-375.

[20] Kim TO, Cheung GSP, Lee JM, Kim BM, Hur B, Kim HC. Stress distribution of three Ni-Ti rotary files under bending and torsional conditions using a mathematic analysis. Int Endod J, 2009; 42:14-21.

[21] Kim HC, Kim HJ, Lee CJ, Kim BM, Park JK, Versluis A. Mechanical response of nickel-titanium instruments with different cross-sectional designs during shaping of simulated curved canals. Int Endod J, 2009; 42:593-602.

[22] Nagasawa A. A new phase transformation in the Ni-Ti alloy. J Phys Soc Japan, 1970; 29:1386.

[23] Ling HC, Kaplow R. Macroscopic length changes during the B2  R and M  B2 transitions in equiatomic Ni-Ti alloys. Mat Sci Eng, 1981; 51:193–201.

[24] Peixoto IFC, Pereira ES, Silva JG, Viana AC, Buono VT, Bahia MG. Flexural fatigue and torsional resistance of ProFile GT and ProFile GT series X instruments. J Endod, 2010; 36:741-744.

[25] Liu J. Characterization of new rotary endodontic instruments fabricated from special thermomechanically processed Ni-Ti wire (PhD dissertation). Columbus, OH: The Ohio State University; 2009.

[26] Cheung GSP, Darvell BW. Fatigue testing of a NiTi rotary instrument. Part 1: strain-life relationship. International Endodontic Journal, 2007; 40:612-618.

[27] Cheung GSP, Zhang EW, Zheng YF. A numerical method for predicting the bending fatigue life of NiTi and stainless steel root canal instruments. Int Endod J, 2011; 44:357-361.

[28] Lagoudas, DC. Shape Memory Alloys: Modeling and Engineering Applications. Springer Science + Business Media, LLC, NY, USA, 2008.

[29] Darabara ML, Bourithis L, Zinelis S, Papadimitriou. Susceptibility to localized corrosion of stainless steel and NiTi endodontic instruments in irrigating solutions. Int Endod J, 2004; 37:705-710.